Dynamo regimes dependence on the heterogeneous CMB heat flux

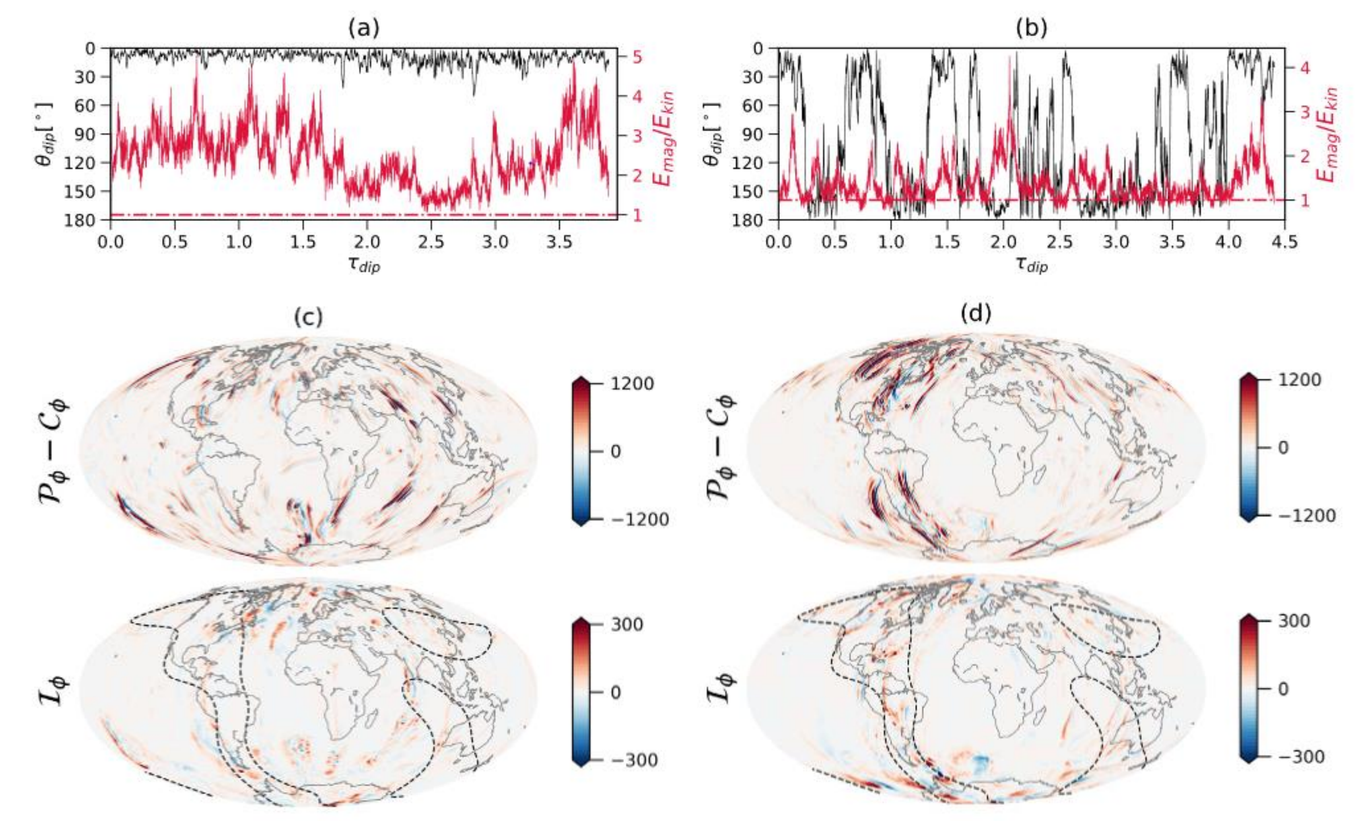

Hagay Amit, Filipe Terra-Nova, Gaël Choblet

Laboratoire de Planétologie et Géosciences, Nantes, France

Strasbourg, July 2025

Dynamo models

Non-dimensional MHD equations for an electrically-conductive, Boussinesq, incompressible fluid in a rotating convecting spherical shell (e.g. Olson and Christensen, 2002):

Navier-Stokes (conservation of momentum):
$$E\left(\frac{\partial \vec{u}}{\partial t} + \vec{u}\cdot\nabla\vec{u} - \nabla^2\vec{u}\right) + 2\hat{z}\times\vec{u} + \nabla P = Ra\frac{\vec{r}}{R}T + \frac{1}{Pm}\left(\nabla\times\vec{B}\right)\times\vec{B}$$

Induction (Maxwell's equations of electromagnetism):
$$\frac{\partial \vec{B}}{\partial t} = \nabla\times\left(\vec{u}\times\vec{B}\right) + \frac{1}{Pm}\nabla^2\vec{B}$$

Heat (conservation of energy):
$$\frac{\partial T}{\partial t} + \vec{u}\cdot\nabla T = \frac{1}{Pr}\nabla^2 T$$

Continuity (conservation of mass):
$$\nabla\cdot\vec{u} = 0$$

No magnetic monopoles:
$$\nabla\cdot\vec{B} = 0$$

Heat flux Rayleigh	$Ra = \frac{\alpha g_0 q_0 D^4}{\upsilon k \kappa}$
Ekman	$E = \frac{\upsilon}{\Omega D^2}$
Prandtl	$Pr = \frac{\upsilon}{\kappa}$
magnetic Prandtl	$Pm = \frac{\upsilon}{\lambda}$

- Thermochemical convection: prescribed CMB flux, fixed ICB temperature, zero co-density sources/sinks.
- No-slip, insulating boundaries.

Dynamo models

Non-dimensional MHD equations for an electrically-conductive, Boussinesq, incompressible fluid in a rotating convecting spherical shell (e.g. Olson and Christensen, 2002):

Navier-Stokes (conservation of momentum): $$E\left(\frac{\partial \vec{u}}{\partial t} + \vec{u}\cdot\nabla\vec{u} - \nabla^2\vec{u}\right) + 2\hat{z}\times\vec{u} + \nabla P = Ra\frac{\vec{r}}{R}T + \frac{1}{Pm}\left(\nabla\times\vec{B}\right)\times\vec{B}$$

Induction (Maxwell's equations of electromagnetism): $$\frac{\partial \vec{B}}{\partial t} = \nabla\times\left(\vec{u}\times\vec{B}\right) + \frac{1}{Pm}\nabla^2\vec{B}$$

Heat (conservation of energy): $$\frac{\partial T}{\partial t} + \vec{u}\cdot\nabla T = \frac{1}{Pr}\nabla^2 T$$

Continuity (conservation of mass): $$\nabla\cdot\vec{u} = 0$$

No magnetic monopoles: $$\nabla\cdot\vec{B} = 0$$

Heat flux Rayleigh	$Ra = \frac{\alpha g_0 q_0 D^4}{\upsilon k \kappa}$
Ekman	$E = \frac{\upsilon}{\Omega D^2}$
Prandtl	$Pr = \frac{\upsilon}{\kappa}$
magnetic Prandtl	$Pm = \frac{\upsilon}{\lambda}$

- Thermochemical convection: prescribed CMB flux, fixed ICB temperature, zero co-density sources/sinks.
- No-slip, insulating boundaries.
- For **heterogeneous CMB heat an additional parameter *q****

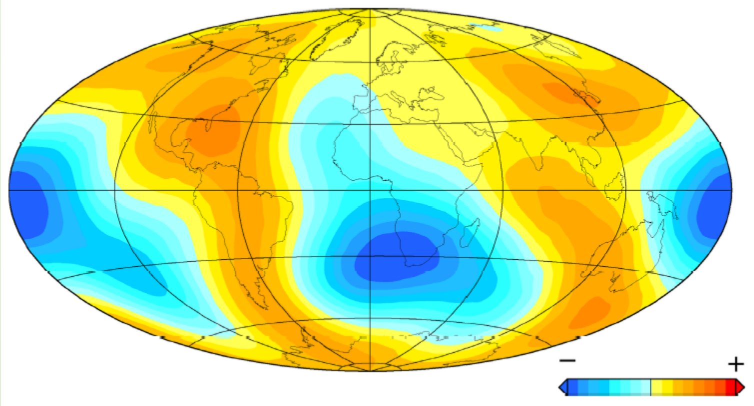

$$q^* = \frac{q_{max} - q_{min}}{2q_0}$$

Dependence on main control parameters - homogeneous boundary conditions

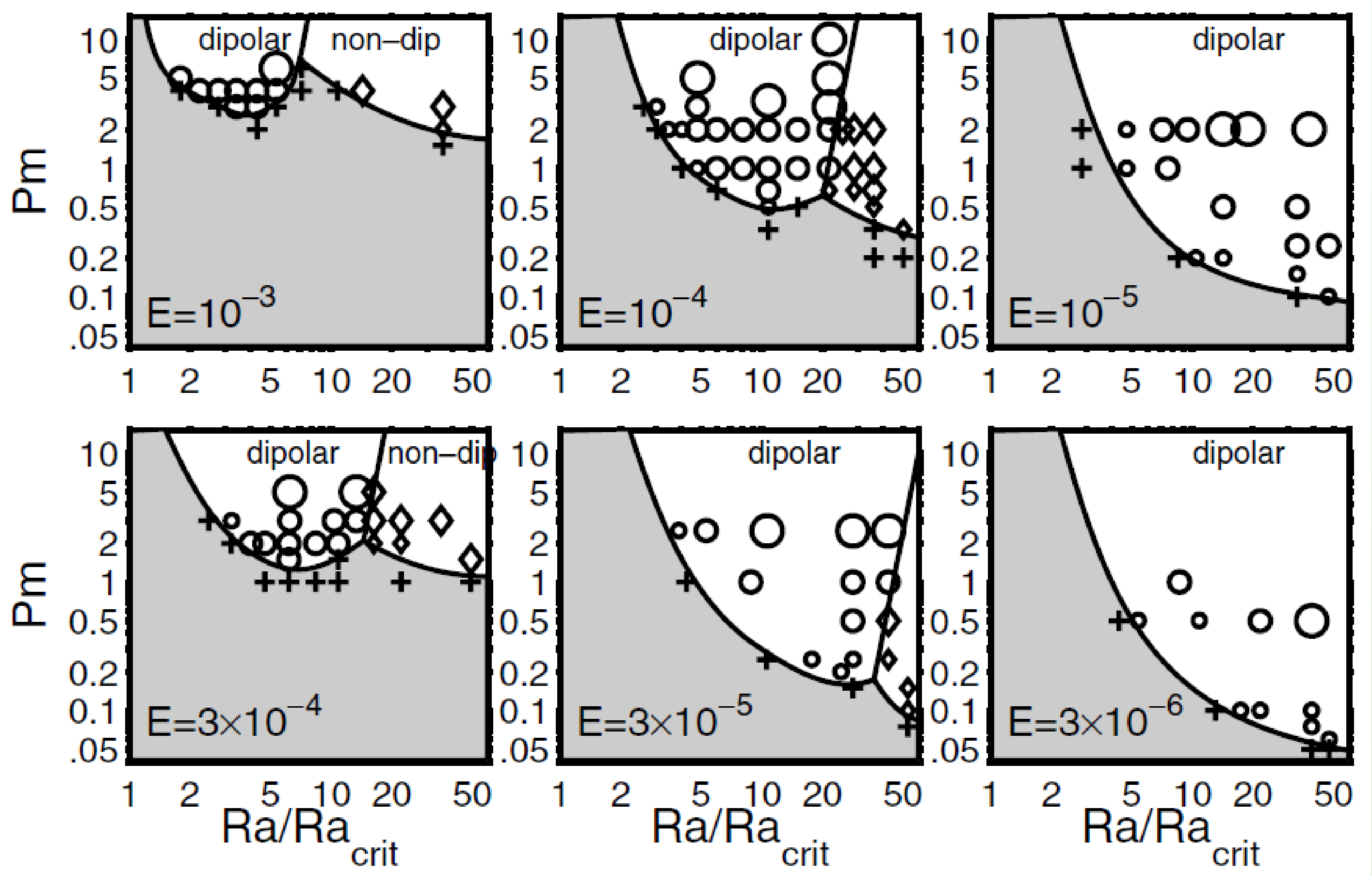

- Transitions (dynamo onset, non-reversing to reversing) established dependencies on main control parameters (e.g. Christensen and Aubert, 2006).
- **Dependence on amplitude of CMB heat flux heterogeneity *q**?**
- Dynamo failure at very large q* (Olson and Christensen, 2002)?

Dynamo models classification

- **Dipole tilt range** for non-reversing/reversing.
- **Critical relative dipolarity** for dipolar/multipolar.

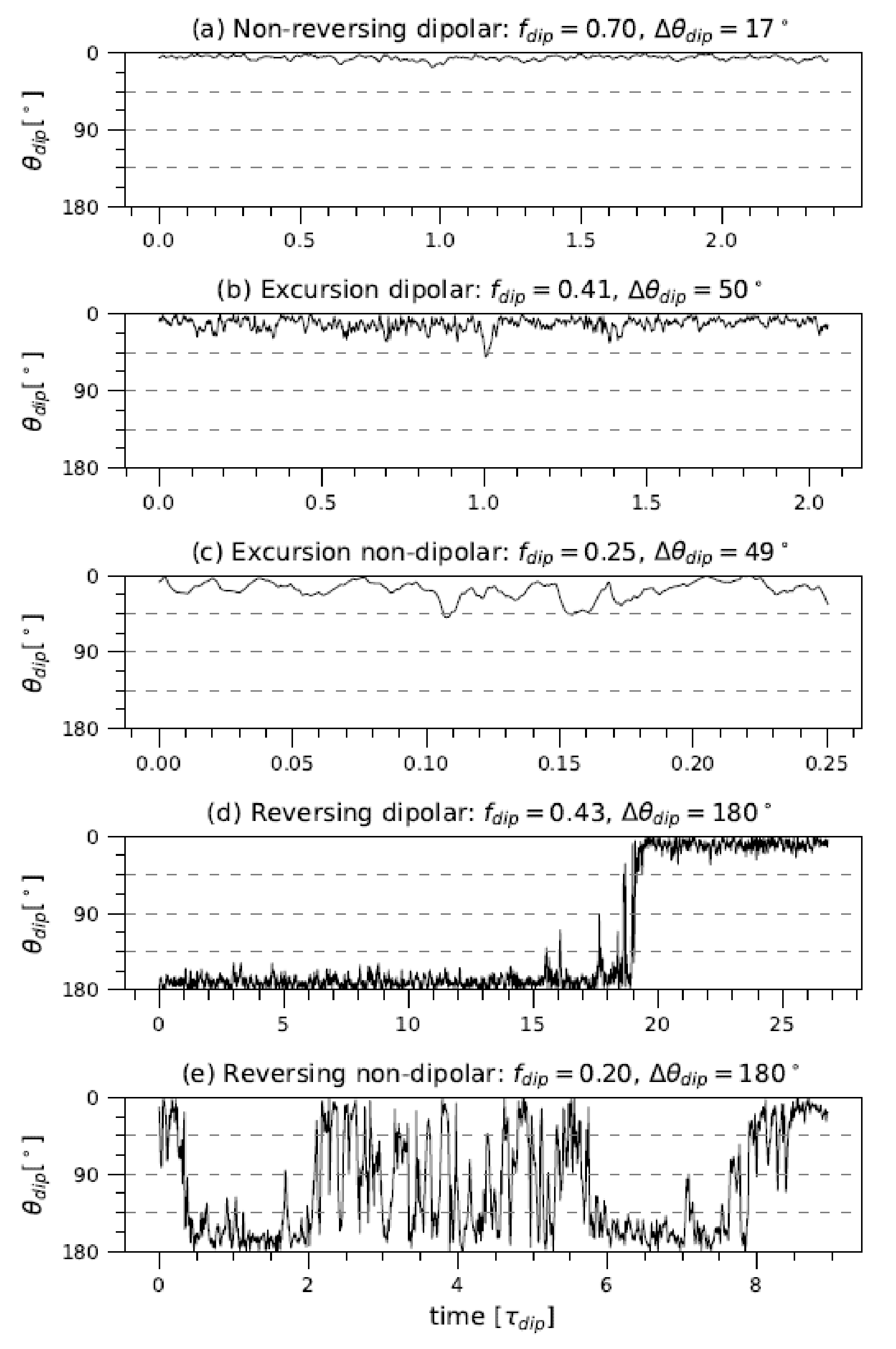

Dynamo models classification

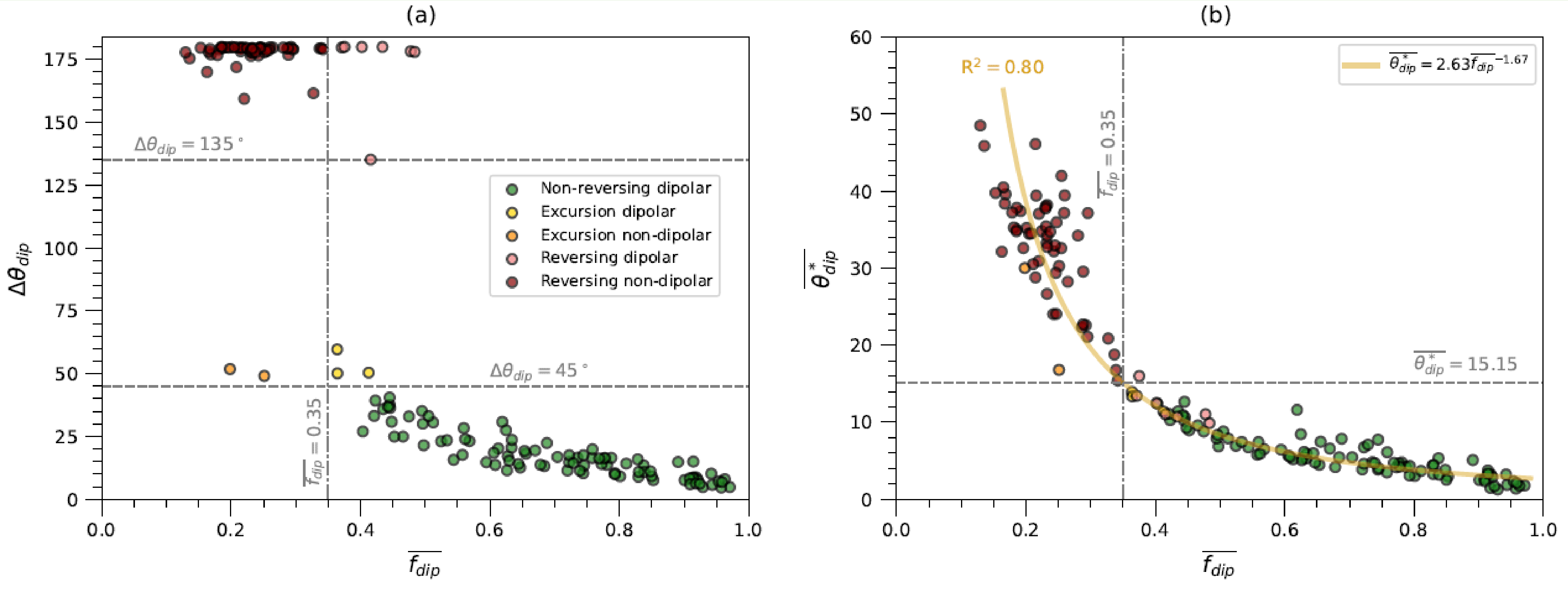

- **Dipole tilt range** for non-reversing/reversing.
- **Critical relative dipolarity** for dipolar/multipolar.
- All non-reversing models are dipolar (green).

- **Distance of dipole axis from north pole** inversely related to relative dipolarity.
- Power law fit intersection with f_{dip}=0.35 => **critical dipole tilt for reversibility.**
- All models above critical dipole tilt exhibit reversals (or excursions) – **predicting reversals** in finite simulation runs.

Dynamo regimes diagrams

- Dynamo regimes vs. convective supercriticality (x-axis) and *Pm* (y-axis) for decreasing *E* (left to right) and increasing *q** (top to bottom).
- Increasing convection destabilizes the dipole, increasing rotation rate stabilizes the dipole, as with homogeneous boundary conditions.
- Reversing dipolar models close to the non-reversing/reversing transition.

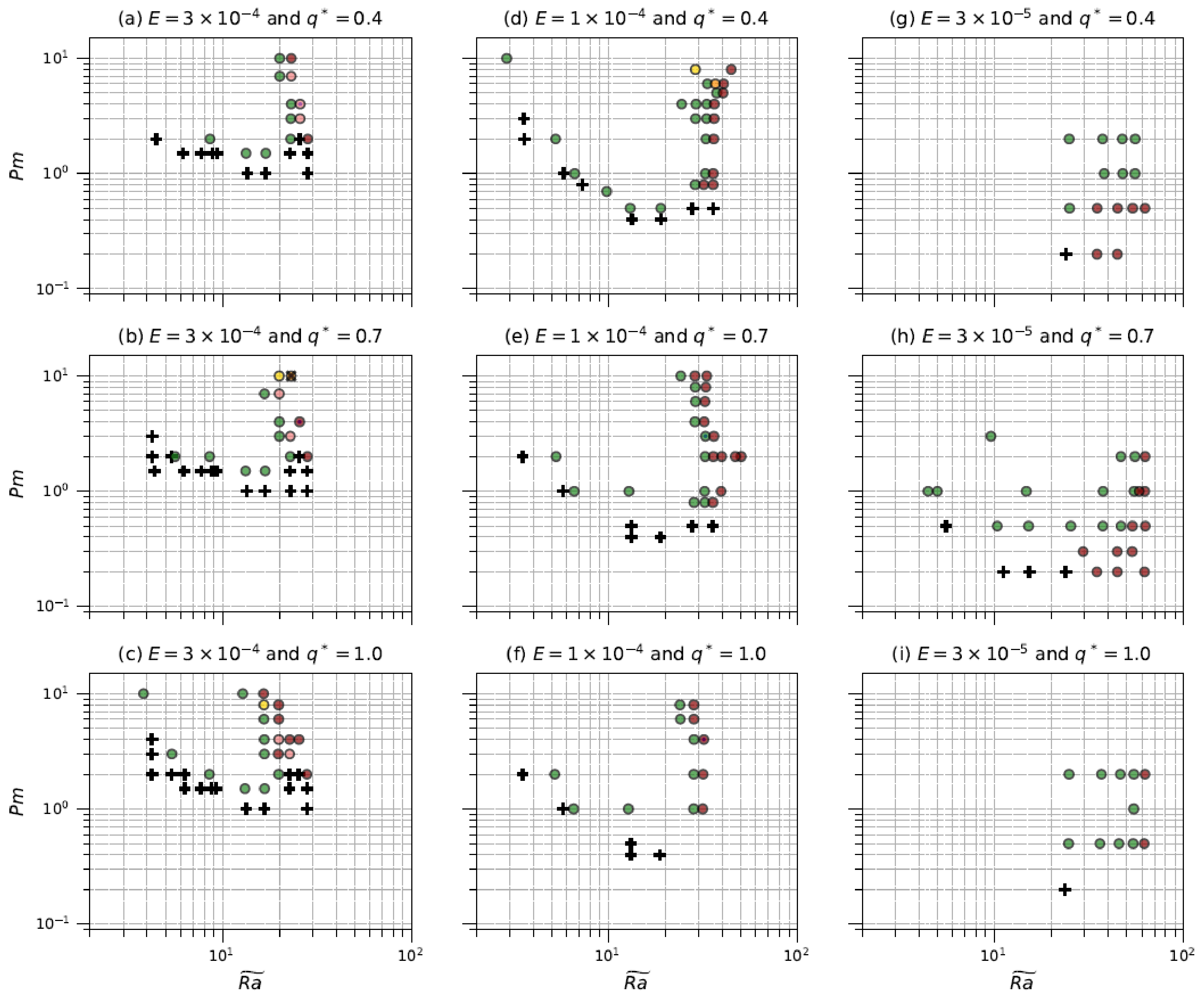

Dynamo regimes diagrams

- Dynamo regimes vs. convective supercriticality (x-axis) and *Pm* (y-axis) for decreasing *E* (left to right) and increasing *q** (top to bottom).
- Increasing convection destabilizes the dipole, increasing rotation rate stabilizes the dipole, as with homogeneous boundary conditions.
- Reversing dipolar models close to the non-reversing/reversing transition.
- **Increasing *Pm* destabilizes the dipole** (in contrast to dynamos with homogeneous boundary conditions).

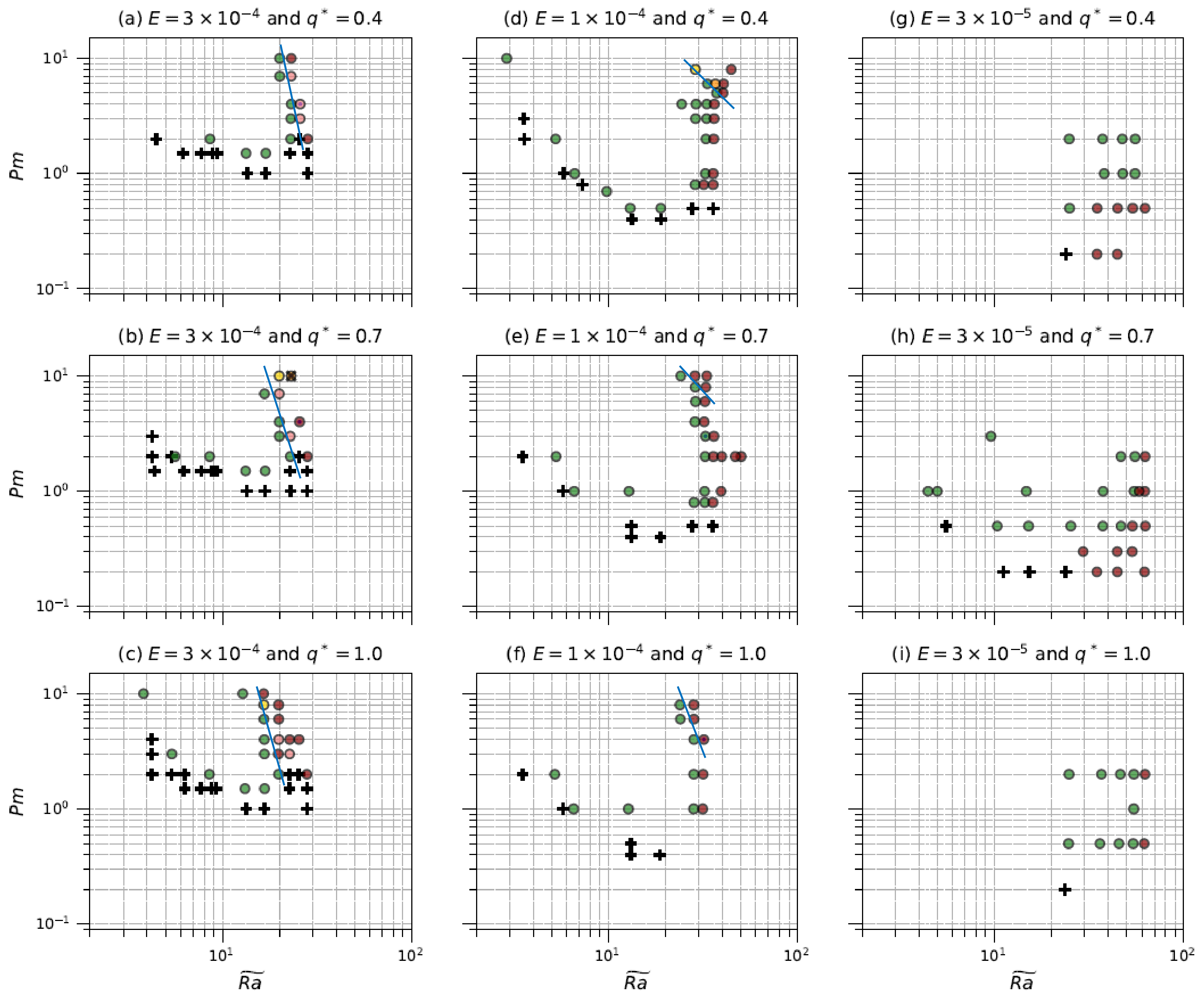

Dynamo regimes diagrams

- Dynamo regimes vs. convective supercriticality (x-axis) and *Pm* (y-axis) for decreasing *E* (left to right) and increasing *q** (top to bottom).

- Increasing convection destabilizes the dipole, increasing rotation rate stabilizes the dipole, as with homogeneous boundary conditions.

- Reversing dipolar models close to the non-reversing/reversing transition.

- **Increasing *Pm* destabilizes the dipole** (in contrast to dynamos with homogeneous boundary conditions).

- At large *Pm* transition to reversals at lower *Ra* with increasing *q** (e.g. a to c or g to i) i.e. boundary **heterogeneity favors reversals**.

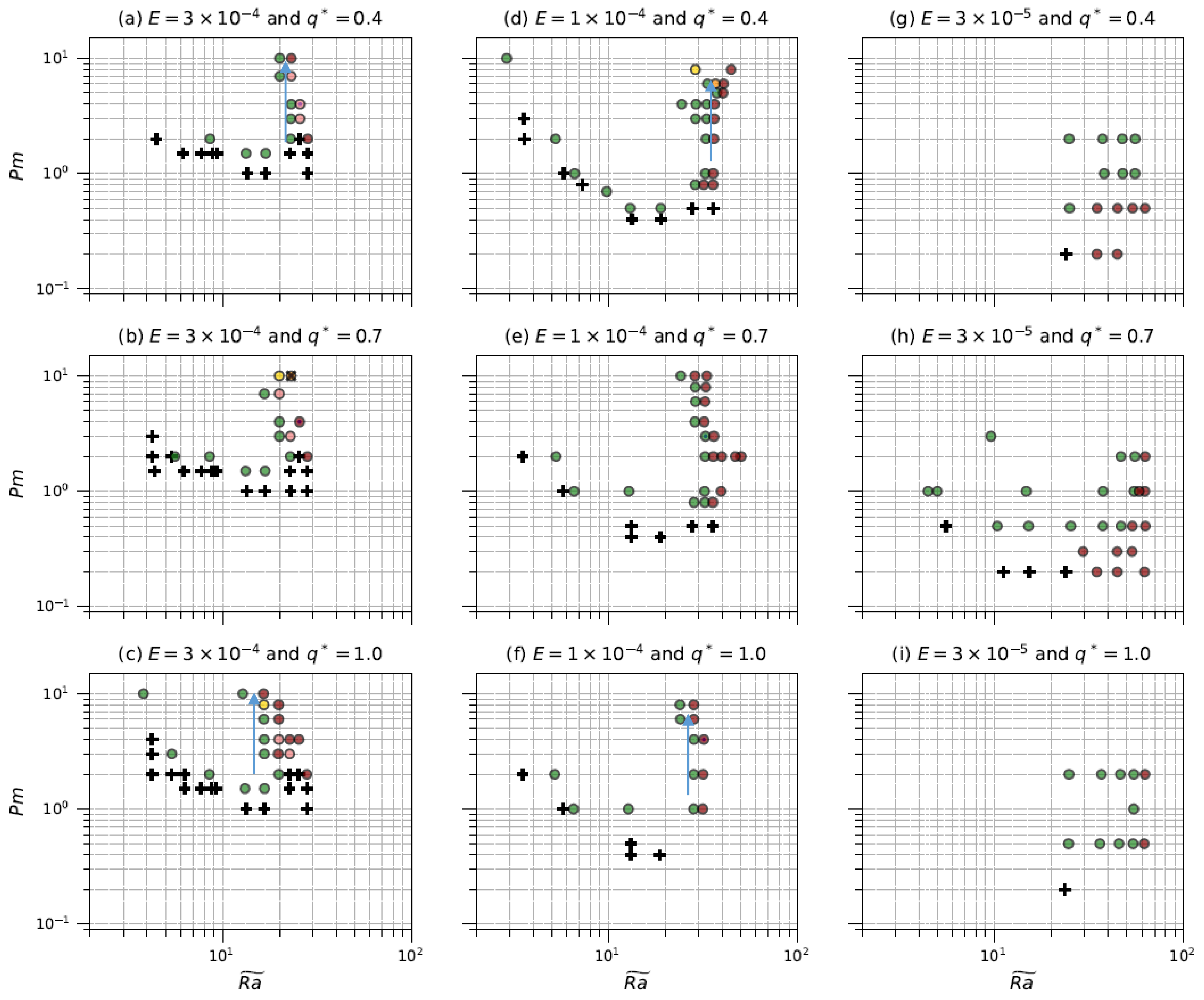

Dependence on *Ra*

- Transition from non-reversing (a) to reversing (b).

Snapshots:
- Significant drop in dipolarity (c and d), see e.g. mixed polarities at high latitudes of the southern hemisphere (d).

Time averages:
- Intense high-latitude flux patches in time-average fields (including reversing case).

- Order 2 signature in non-reversing time-average field, one patch in reversing model.

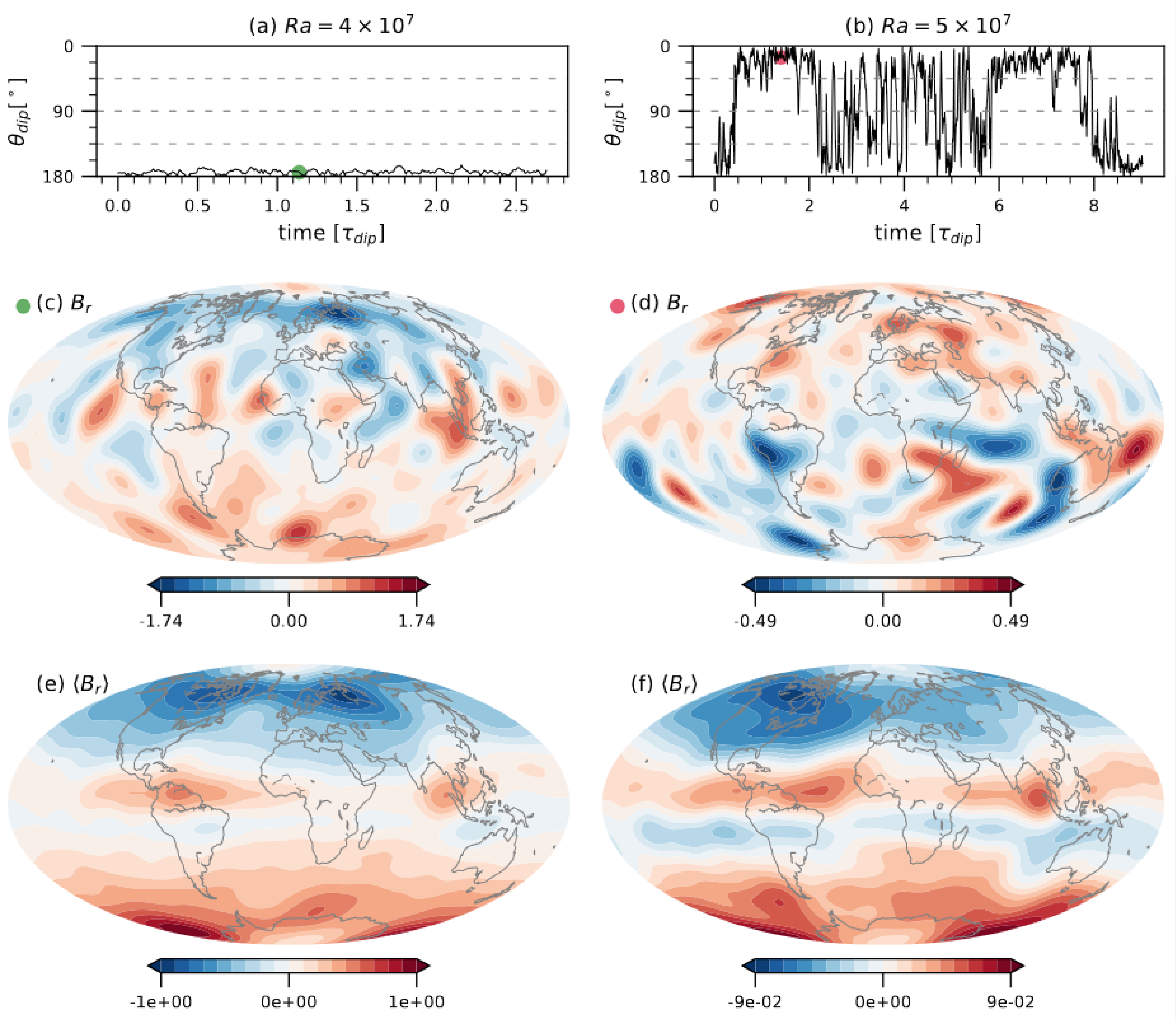

E=1e−4, *Pm*=2, *q**=1.0

Dependence on *q**

- Transition from non-reversing (a) to reversing (b).

Snapshots:

- **Both dipolarities >0.35** (c and d), even slightly larger for the reversing case (d).

Time averages:

- Intense high-latitude flux patches (including reversing case).
- Order 2 signature in non-reversing model, one patch in reversing model.
- **Larger amplitude of northern polar minimum** (Lézin et al., 2023).

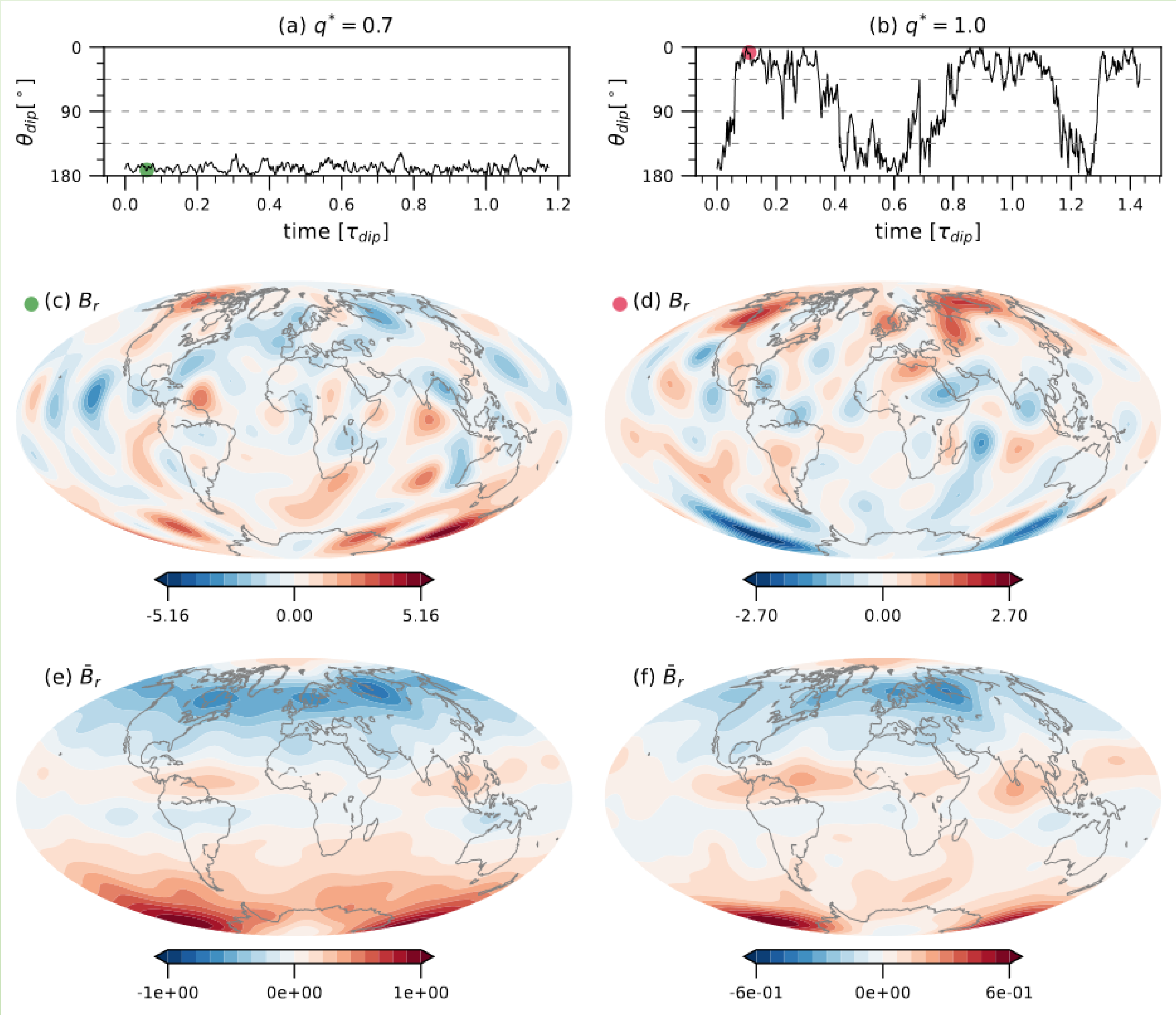

E=1e−4, *Ra*=4e7, *Pm*=8

Dependence on *Pm*

- **Non-trivial transition** from non-reversing (a) to reversing (b).

Snapshots:

- Both dipolarities >0.35 (c and d), but significantly lower for the reversing case (c).
- Increasing **boundary-driven equatorially symmetric field** in large Pm model reduces dipolarity (e.g. below Indian Ocean in d).

Time averages:

- Intense high-latitude flux patches (including reversing case).
- Order 2 signature in non-reversing model, one patch in reversing model.
- Larger amplitude of northern polar minimum (Lézin et al., 2023).

E=1e−4, Ra=4e7, q^*=1.0

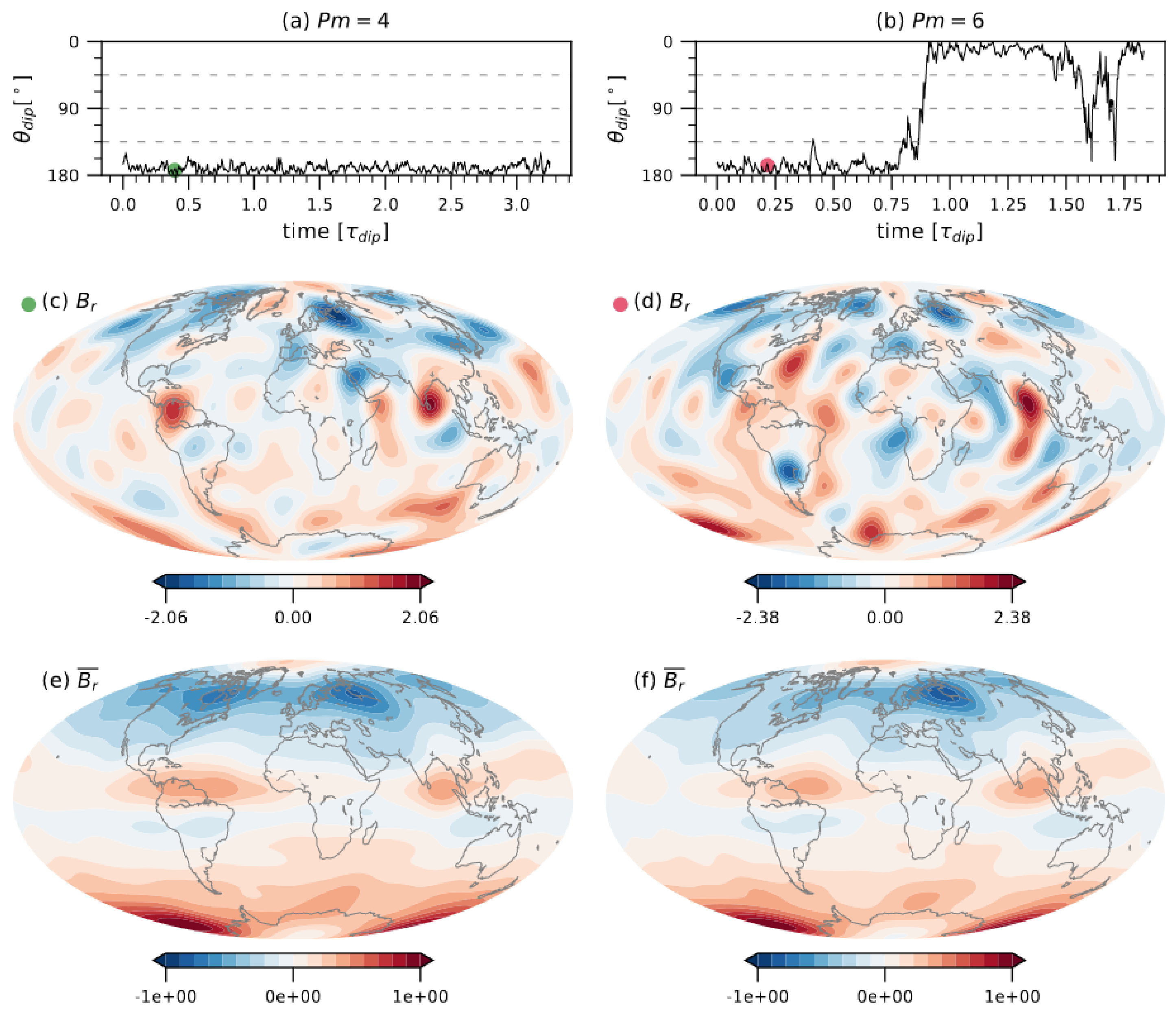

Dynamical origin

- Dynamics concentrated inside TC in non-reversing model, **more balanced inside/outside TC dynamics in reversing** model.
- Striking **hemispherical co-density outside TC** in both cases driven by southern centers of LLSVPs.
- **Strengthenning of downwellings below the Americas and east Asia in the reversing model** – decreasing role of TC downwellings which maintain the axial dipole (e.g. Christensen et al., 1998) causes reversals.

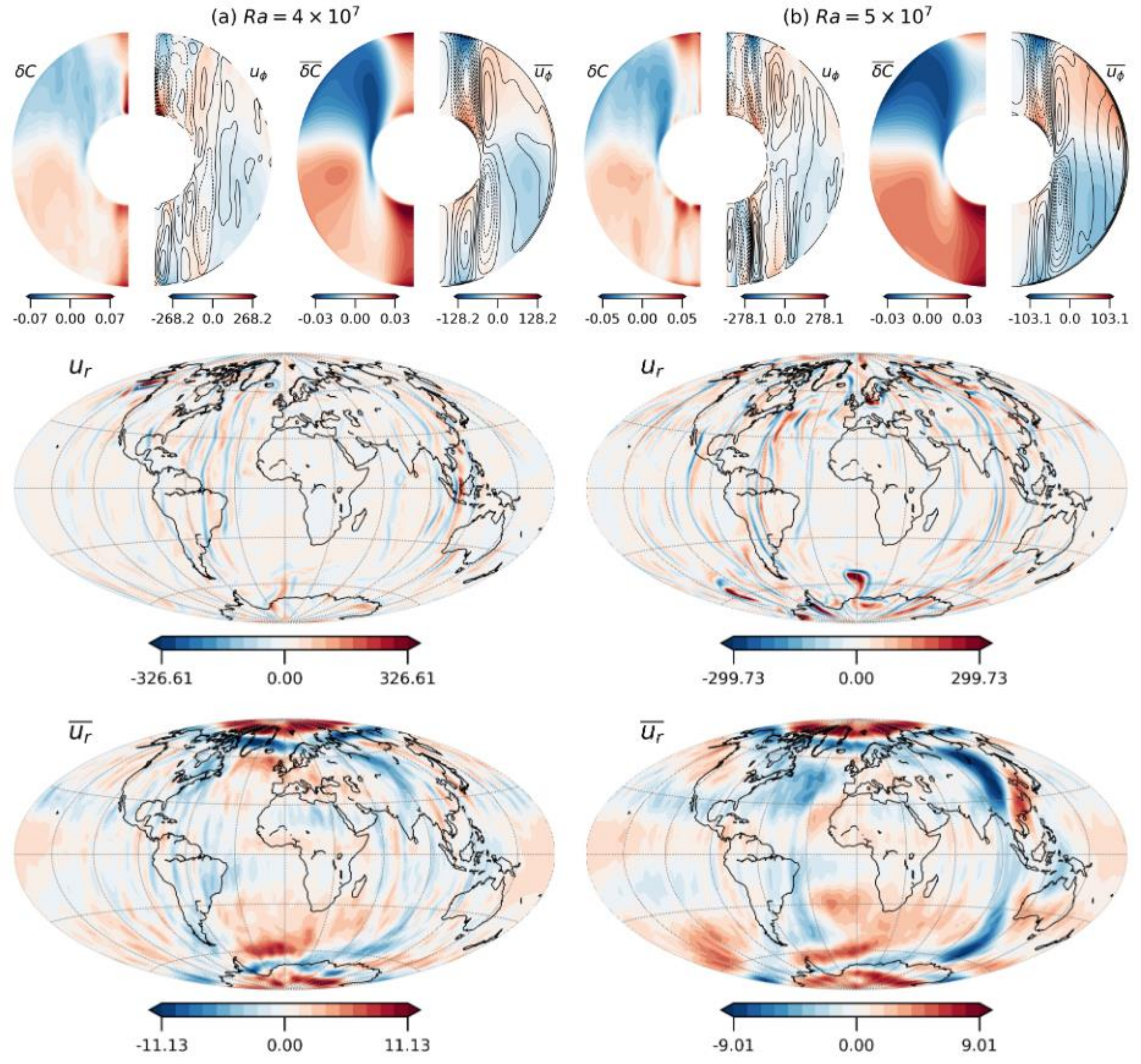

Determining parameter for the dipolar to reversing transition

- **Local Rossby number** (Olson and Christensen, 2006) and **magnetic to kinetic energy ratio** (Schwaiger et al., 2019) separate most models but not all.
- **Heterogeneity-corrected** corresponding quantities (Olson and Amit, 2014).
- Increase/decrease in heterogeneity-corrected local Rossby number for reversing/non-reversing dynamos and decrease/increase in heterogeneity-corrected energy ratio for reversing/non-reversing dynamos with increasing *q**.
- Inertial control: **Regional triggering of reversals** (Terra-Nova and Amit, 2024).
- Geographical control: Large heat flux at high latitudes stabilizes the dipole.

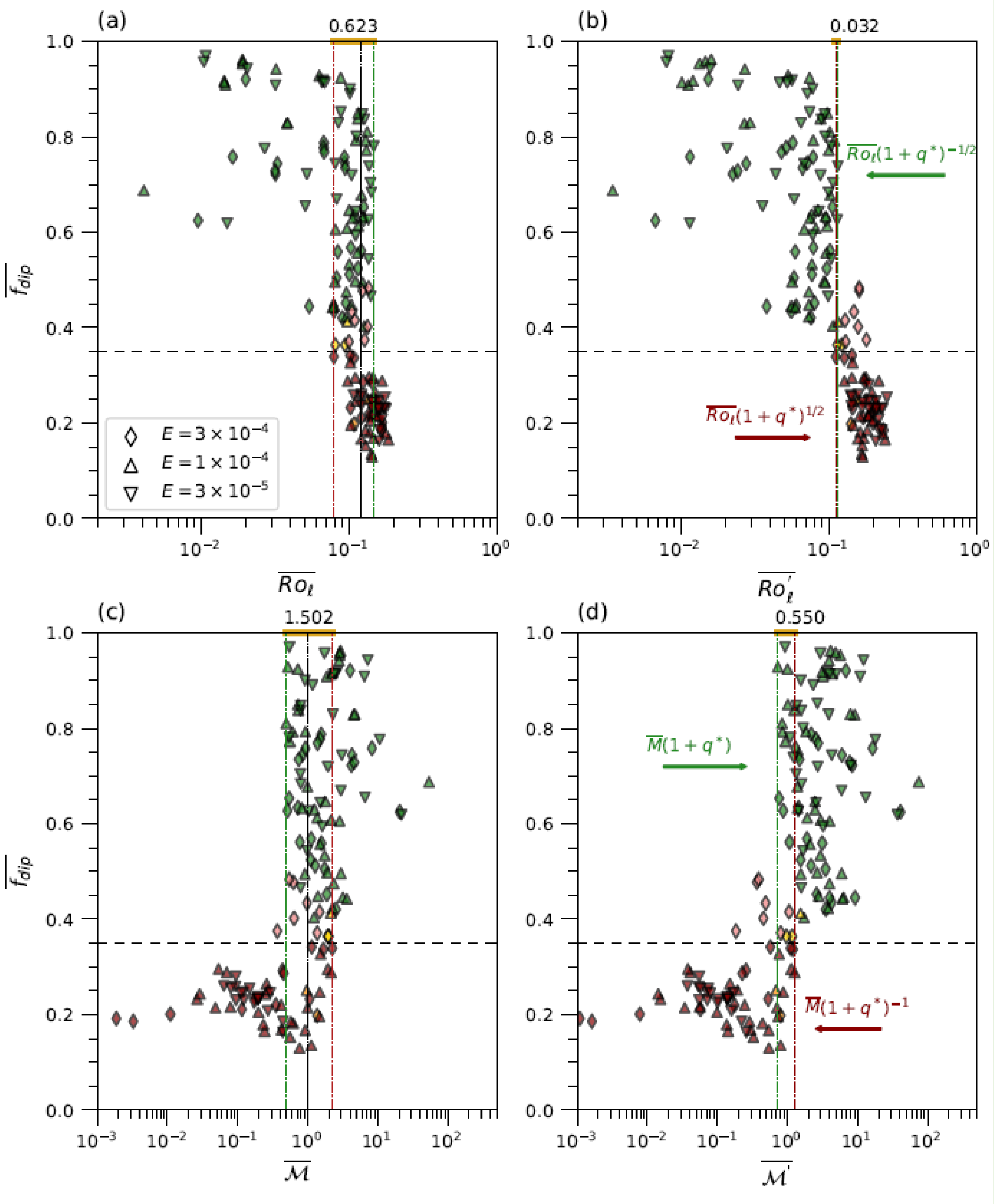

Determining parameter for the dipolar to reversing transition – temporal variability

Accounting for temporal variability only weakly reduces the overlap for both the local Rossby number and the energy ratio.

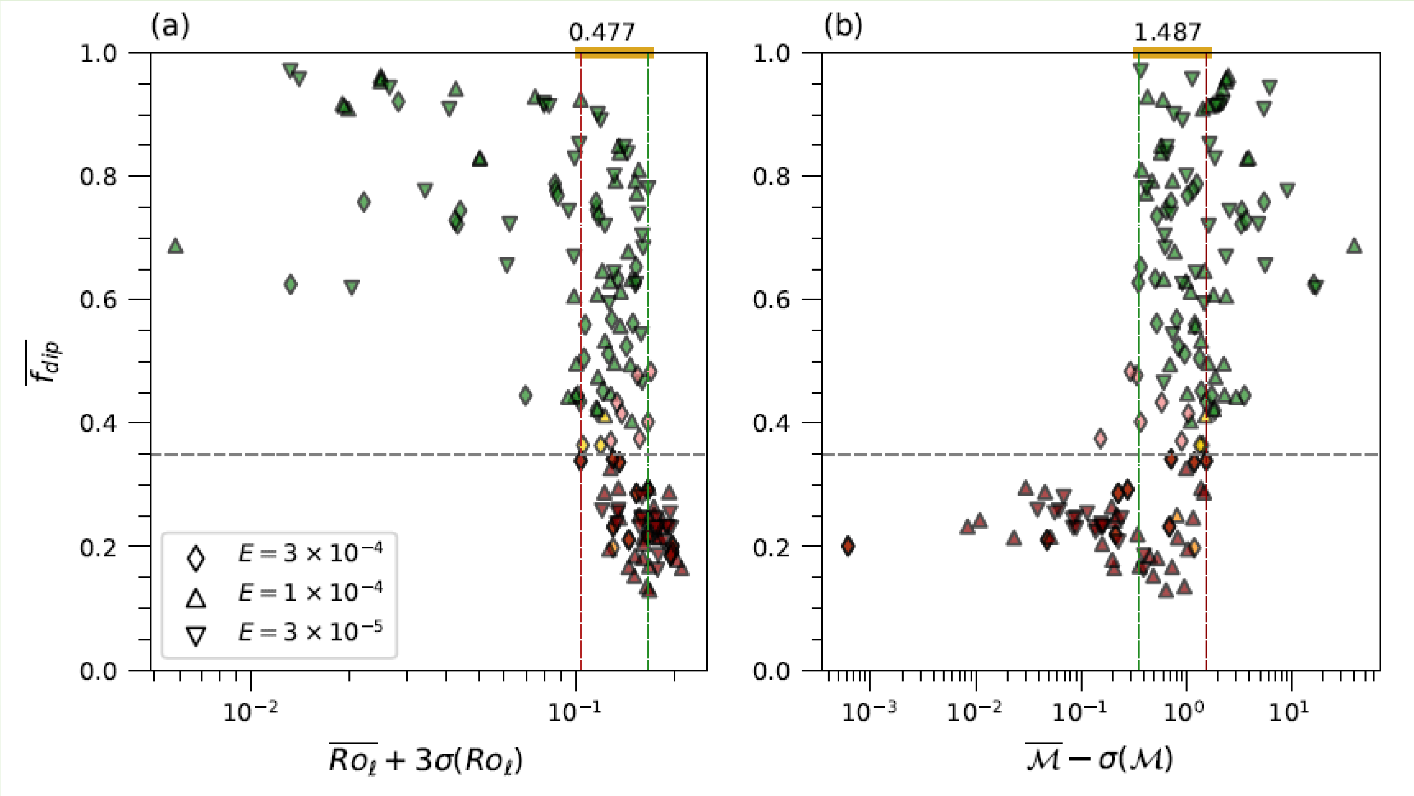

Determining parameter for the dipolar to reversing transition – equatorial symmetry

- Relative dipolarity **linearly** related to **modified zonal anti-symmetric energy ratio** (Frasson et al., 2025).
- But still overlap…
- Reversing dipolar and excursions dipolar models confined to a narrower range of modified energy ratios (black vertical lines) than of Frasson et al. (2025) (grey box) – effect of tomographic vs. distinctive outer boundary heat flux patterns.

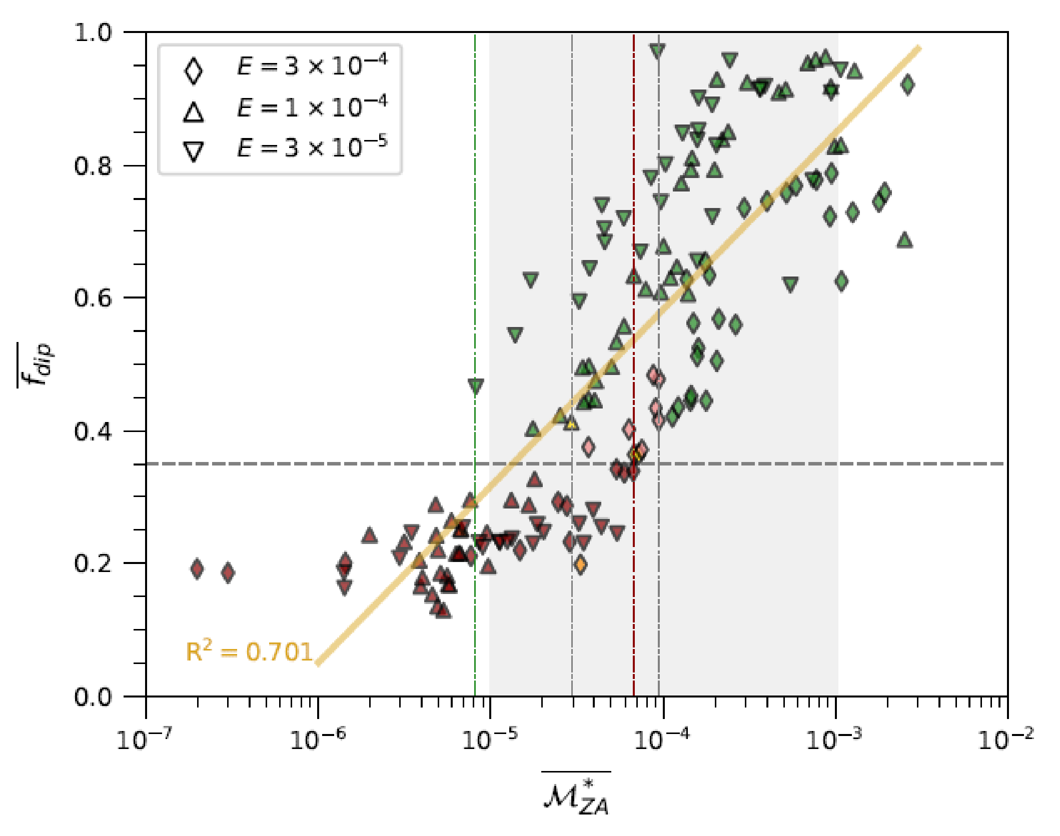

Pm dependence and boundary-driven equatorially anti-symmetric convection

- Convection = “homogeneous” dynamo + boundary-driven.
- “homogeneous” dynamo: Small-scale (turbulent) equatorially symmetric (rapid rotation effects) convection.
- Boundray-driven: Large-scale mixed symmetric/anti-symmetric (tomographic) convection.
- Increasing Pm filters small-scale convection (Yadav et al., 2016; Schwaiger et al., 2019) => affects more “homogeneous” dynamo => increase in relative equatorially anti-symmetric convection.

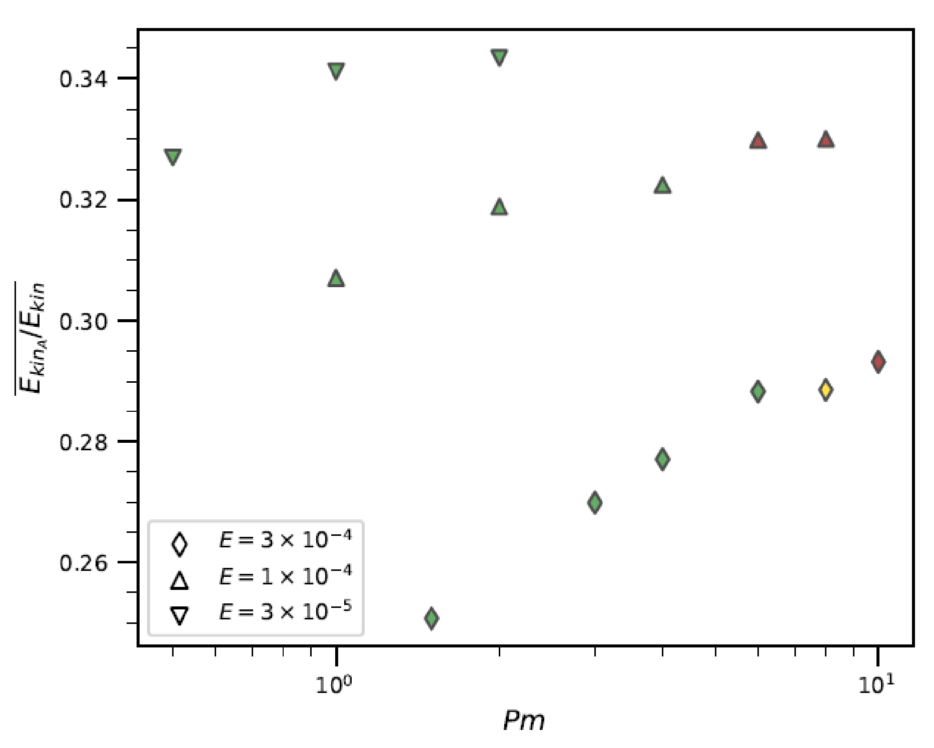

Discussion – boundary-driven convection inside/outside TC and equatorial symmetry

- **Axial dipole** maintained by intense magnetic **flux patches** at the edge of the **TC**.
- **Boundary-driven convection outside TC** reduces relative intensity of TC downwellings => reversals.
- **Boundary-driven anti-symmetric convection** => reversals.

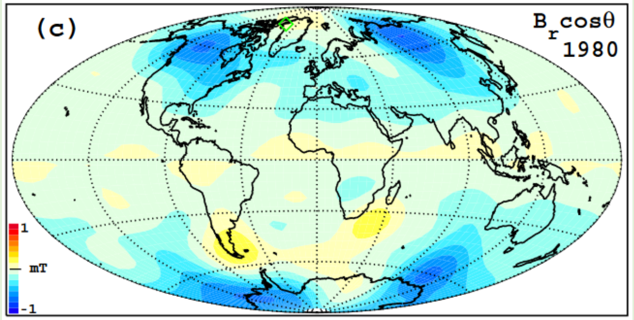

Spatial contributions to the geomagnetic axial dipole. From Olson and Amit (2006).

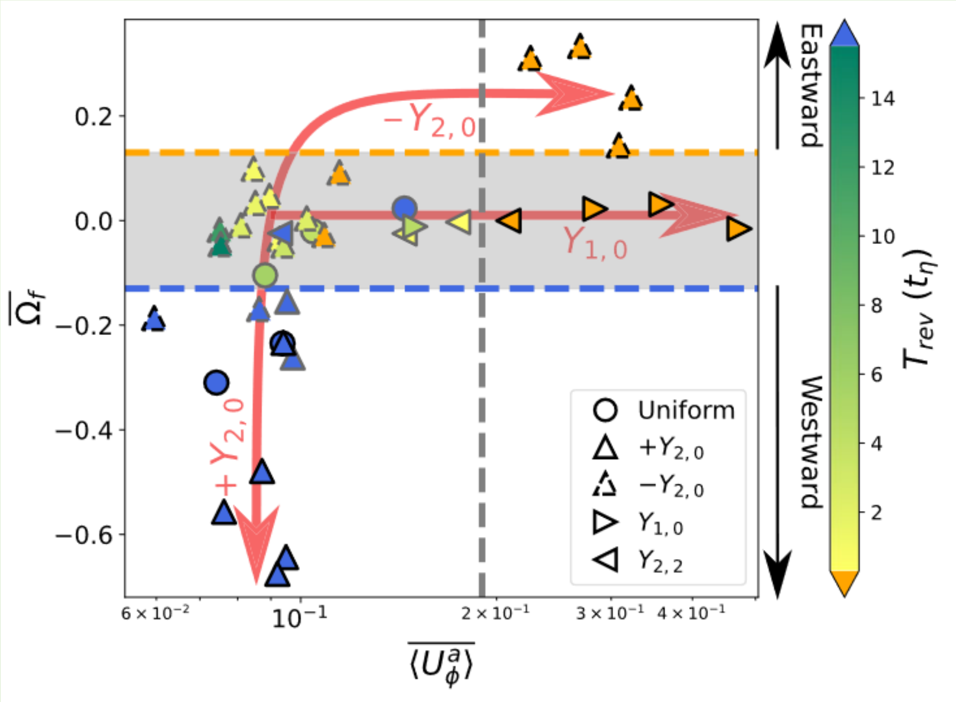

Impact of equatorial symmetry of the flow on the reversibility of dynamo models. From Frasson et al. (2025).

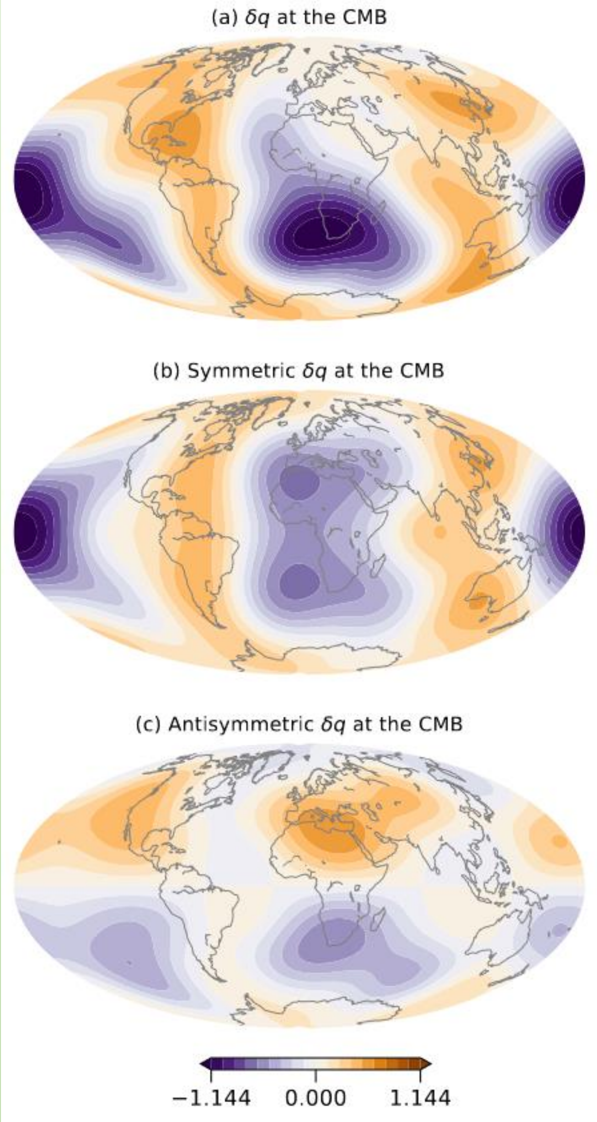

Discussion – dynamo regimes *Pm* dependence with tomographic CMB heat flux

- Increasing Pm **diffuses small-scale convection** (Yadav et al., 2016).
- With homogeneous boundary conditions => small-scale equatorially symmetric convection.
- With tomographic CMB heat flux => relatively **large-scale** partly **anti-symmetric** boundary-driven **convection**.
- Increasing Pm with tomographic CMB heat flux increases equatorial anti-symmetry of convection => reversals!

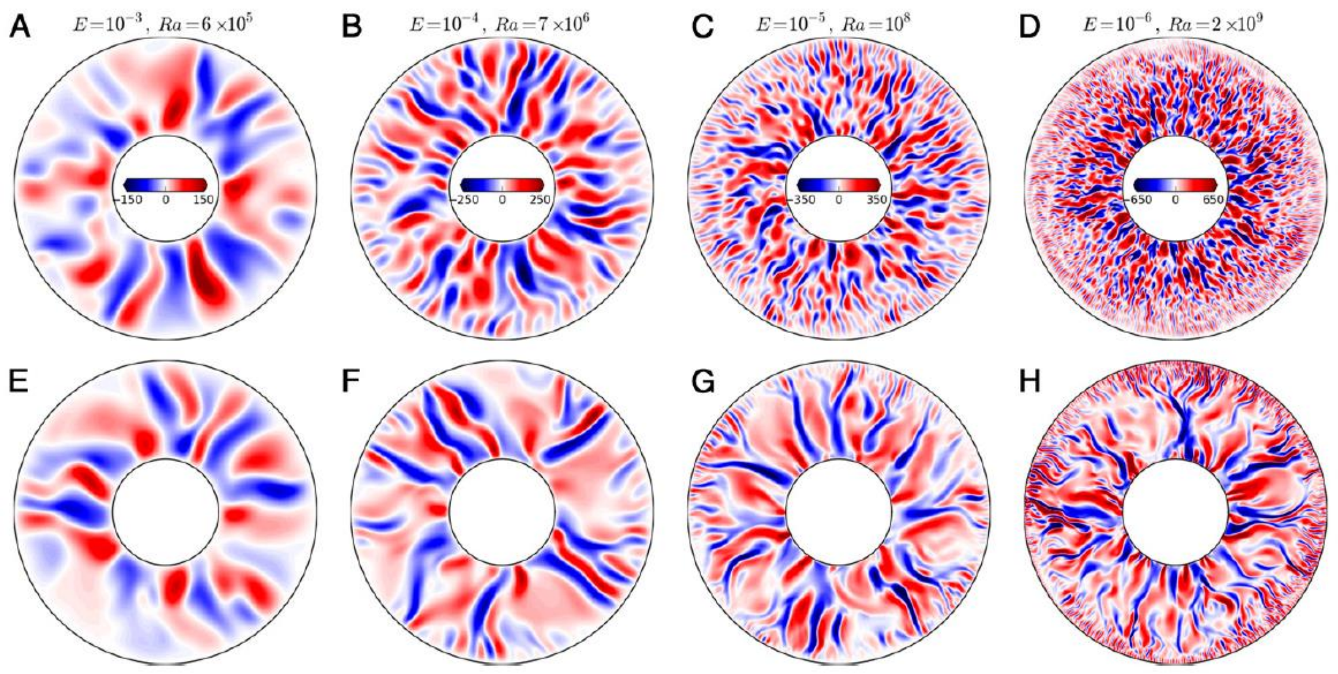

Radial velocity in the equatorial plane for non-magnetic (top) and dynamo (bottom) models. From Yadav et al. (2016).

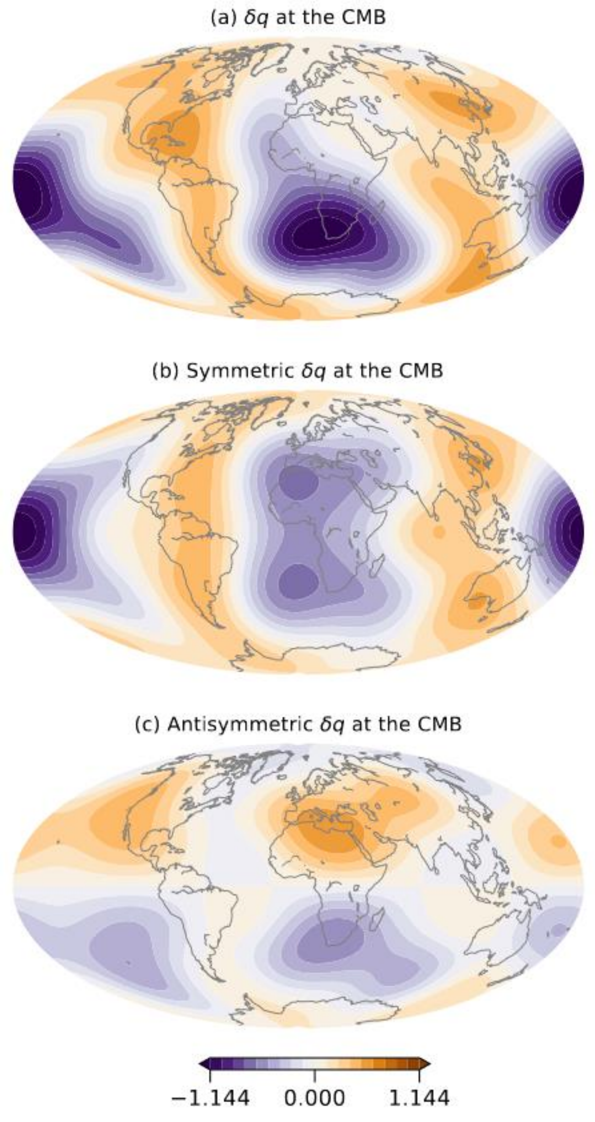

Dynamo regimes dependence on the heterogeneous CMB heat flux – conclusions

Classification and regimes diagrams:

- Dynamo models with a time-average dipole tilt >15 degrees will reverse.
- Increasing *Ra* promotes reversals, decreasing *E* stabilizes the dipole.
- Increasing *Pm* favors reversals! Filtering of small-scale equatorially-symmetric “homogeneous” dynamo convection.
- Increasing *q** favors reversals for moderate *q** (Terra-Nova and Amit, 2024).

Boundary-driven convective morphology:

- Tomographic CMB heat flux increases convection outside TC => reduction of TC downwellings favor reversals.
- Tomographic CMB heat flux induces thermal hemisphericity outside TC => anti-symmetric convection favors reversals.

Determining parameters for the transition:

- Local Rossby number and magnetic energy ratio separate most non-reversing/reversing dynamo models but some overlap lingers.
- Boundary heterogeneity corrected parameters:
    - Inertial control: *q** dependence indicates regional triggering of reversals.
    - Geographic control: Large CMB heat flux at high latitudes stabilizes the dipole.
- Confirmed linear relation between relative dipolarity and modified energy ratio (Frasson et al., 2025), but non-reversing/reversing models still overlap.